



In situ photoacoustic measurement of soot profiles in laminar flames using a high-repetition-rate pulsed fibre laser

Gordon S. Humphries^{1,2} · Robert Roy¹ · John D. Black¹ · Michael Lengden² · Iain S. Burns¹

Received: 10 January 2019 / Accepted: 5 March 2019
© The Author(s) 2019

Abstract

We present a photoacoustic technique for in situ sensing of particulates in reacting flows. The method is demonstrated by measuring soot distribution in laminar flat flames. The excitation source is a high-repetition-rate pulsed fibre laser. The resulting acoustic signals are measured using a uni-directional microphone and lock-in amplifier. Based on an Allan–Werle plot, the detection limit is estimated to be a soot volume fraction of 3 parts-per-billion. Fluence curves are presented, showing a plateau region similar to the behaviour typically observed for laser-induced incandescence. A dependence of the photoacoustic signal on pulse repetition rate is also demonstrated.

1 Introduction

Despite the increased use of renewable energy sources, the combustion of hydrocarbon fuels is expected to continue as one of the major sources of energy generation for at least the next few decades [1]. Polycyclic aromatic hydrocarbons (PAH) and soot formed during incomplete combustion of such fuels are major sources of global pollution, having detrimental effects both on public health [2] and on the global climate [3]. The accurate measurement of soot in laboratory flames with simple geometries is an important step towards understanding its formation and growth, and is also key to the development and validation of soot formation models [4]. Likewise, practical instruments capable of sensitive measurement of particulates in industrial systems are of relevance to process control and emission reduction.

Laser-induced incandescence (LII) [5] is one of the most commonly used methods for the in situ measurement of soot distribution in flames. Typically, the laser sources used for LII are pulsed lasers with high peak power and pulse durations of roughly 10 ns. The high-fluence irradiation heats the

soot particles to near their sublimation temperature (≈ 4000 K [6]) and detection of the resulting incandescence provides a measure of soot volume fraction. Soot particle size can also be inferred from the rate of particle cooling based on heat transfer models [7].

We have previously demonstrated photoacoustic measurement of soot in flames [8]. Advantages of this approach include the simplicity of the signal collection and the ease of alignment. A pressure wave is generated from the heating and expansion of the surrounding bath gas as soot particles cool following laser heating and can be measured with a suitable microphone or transducer. It should be noted that a disadvantage of the photoacoustic measurement approach is the inherent path-integrated nature of the technique. However, it may be possible to overcome this disadvantage in the future by the use of tomographic measurement approaches. The optical source used in this previous work was a high-power, continuous-wave laser diode. The results showed good agreement with soot profiles measured using LII in the same flames. Nevertheless, the sensitivity was limited by the low amplitude of the laser power modulation at high frequency due to the finite bandwidth of the laser current driver.

A light source capable of a much larger modulation amplitude would, therefore, offer improved sensitivity. Recently, LII measurements have been made using high-repetition-rate pulsed fibre lasers [9]. Pulsed fibre lasers are potentially a more appropriate light source for photoacoustic measurements because there is an effective on–off modulation at kHz rates, which leads to the prospect of a more favourable

✉ Gordon S. Humphries
gordon.humphries@strath.ac.uk

¹ Department of Chemical and Process Engineering,
University of Strathclyde, 75 Montrose St,
Glasgow G1 1XW, UK

² Department of Electronic and Electrical Engineering, Centre
for Microsystems and Photonics, University of Strathclyde,
204 George St, Glasgow G1 1XW, UK

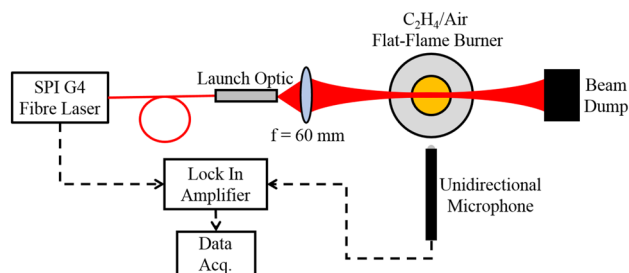


Fig. 1 Experimental setup (red lines denote optical fibre connections, dashed black lines denote electrical connections)

detection limit and sufficient signal levels to characterise the technique further by obtaining fluence curves and investigating measurement stability and frequency response. We present here, to the best of our knowledge, the first measurements of soot distribution using the in situ acoustic response of soot particles heated by a high-repetition-rate pulsed laser.

2 Experimental setup

The experimental setup is shown in Fig. 1. The flat-flame burner used for this work has been described in detail previously [8, 10], consisting of a 33-mm-diameter sintered stainless steel porous plug, with a 38-mm-diameter stainless steel stabilisation plate positioned 21 mm above the surface of the burner. The entire burner assembly can be vertically translated, with respect to the optical components, allowing measurements to be taken at a range of positions above the surface of the burner. All measurements reported here were recorded in premixed flames of ethylene and air. The flow rate of each gas was controlled using mass flow controllers (Cole-Parmer). This enabled the burner to be operated at a range of different fuel equivalence ratios, producing flames which ranged from those with a relatively low soot volume fraction, through to highly sooting conditions ($\phi = 2.1$ to $\phi = 2.48$). The one-dimensional character of these flames should ensure that any errors arising from the path-integrated nature of the photoacoustic technique are relatively minor.

The optical source was a commercially available (SPI Lasers redENERGY G4 20W EP-Z), high-repetition-rate, pulsed fibre laser, emitting at a wavelength of 1060 nm. The pulse repetition rate and drive current were controlled via a PC interface. The divergent output beam from the in-built fibre-launch optic was focussed at the centre of the burner using a 60-mm-focal length, plano-convex lens. The beam profile was measured using a two-axis knife-edge profiler (Thorlabs, BP209-IR/M) and was found to have a waist ($1/e^2$ diameter) of $190\ \mu\text{m}$ at the focus. The diameter of the beam was measured to increase to $250\ \mu\text{m}$ at the outer

circumference of the burner. The measured transverse beam profiles were close to Gaussian and did not vary significantly as a function of pulse energy or repetition rate.

The acoustic signal was detected using a uni-directional condenser microphone (Sennheiser, ME-66), which has a frequency sensitivity range of 40 Hz–20 kHz. A lock-in amplifier (Perkin-Elmer, 7280) was used to measure the amplitude of the acoustic signal at the pulse repetition frequency of the laser. A time constant of 2 s was chosen for lock-in detection to minimise the effect of any slight, short-term disturbances at the periphery of the flame during the measurement. The output from the lock-in amplifier was digitised either using an oscilloscope (Tektronix, TDs3014B), or PCI-based data acquisition card (National Instruments, PCI-6120).

3 Results and discussion

Figure 2 shows the measured photoacoustic signal as a function of laser fluence for 5 kHz, 10 kHz, and 15 kHz laser repetition rates. The fluence is defined here based on the $1/e^2$ beam diameter at the focus. These measurements were recorded at a position 15 mm above the surface of the burner in a $\phi = 2.1$ flame. The background acoustic signal was measured for each laser fluence with the flame extinguished and has been subtracted from each measurement. This background acoustic signal is probably due to laser heating of the optical components and power meter, and is, therefore, minimised by the use of a directional microphone. The 5 kHz and 15 kHz measurements have been normalised to the 10 kHz measurement scale using the manufacturer-stated frequency response curve for the microphone element. The error bars show the standard error calculated from four repetitions of each data point.

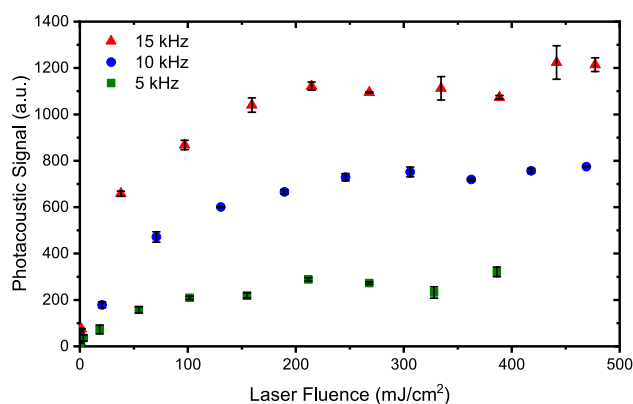


Fig. 2 Measured acoustic signal as a function of laser fluence at various pulse repetition rates, recorded 15 mm above the burner surface in a $\phi = 2.1$ flame. The background acoustic signal has been subtracted

At all three pulse repetition rates, the photoacoustic signal increases with laser fluence, until reaching a plateau at a fluence of approximately 200 mJ cm^{-2} . It is worth noting the similarity in this behaviour to what has been widely observed when measuring peak LII signals as a function of laser fluence [6]. The presence of a plateau tends to indicate that the soot particles are heated to near their sublimation temperature and, therefore, increased fluence does not increase the peak temperature of the soot particles and hence there is no further increase in the measured photoacoustic signal. Interestingly, the signal level of this plateau increases significantly as the pulse repetition rate is increased.

This is explored further in Fig. 3, which shows the acoustic signal as a function of pulse repetition rate. Again, all measurements were corrected using the manufacturer-stated microphone frequency response. The average laser power recorded on the thermal power meter for each measurement is shown on a secondary axis. It is a characteristic of the laser that the peak pulse energy increases with the repetition rate (at a constant drive current setting). Therefore, the laser drive current was fixed at a relatively high level for all these measurements to ensure the measurements were taken in the plateau region of the fluence curve for all the rep-rates tested. A linear trend of increasing acoustic signal with pulse repetition-rate is observed.

In attempting to account for this effect, we note that soot particles will be subject to multiple excitation cycles as they pass through the measurement volume. For example, given an approximate gas velocity of 0.5 ms^{-1} the particles will experience approximately 2, 4, and 6 heating cycles for 5 kHz, 10 kHz, and 15 kHz, respectively. Although the timescale for heat transfer from the soot particle to the surrounding bath gas is typically of the order of a few hundred nanoseconds [6], the bath gas remains at an elevated temperature for a much longer period of time [11]. This build-up of thermal energy in the surrounding bath gas as it passes

through the measurement volume is expected to have some influence on the signal generation.

A further explanation for the observed dependence of photoacoustic signal on repetition rate is based on the duty cycle of the laser excitation. The laser pulses are rather short in duration ($\sim 200 \text{ ns}$) and the heat transfer from the soot particles to the surrounding gas is rapid. This may be expected to result in a fast pressure wave, much shorter in duration than the time between laser pulses. This would lead to a microphone response that is far from sinusoidal, and whose spectrum, therefore, contains significant contributions at higher harmonic frequencies. As the laser repetition rate is increased, the duration of the initial pressure wave will represent a larger fraction of the time between laser pulses, presumably leading to a response with a larger amplitude at the fundamental frequency, in keeping with the trends seen in Figs. 2 and 3.

To illustrate this point, Fig. 4 shows a fast Fourier transform (FFT) of the raw microphone output for a pulse repetition frequency of 10 kHz and a laser fluence of 362 mJ cm^{-2} , recorded 15 mm above the surface of the burner in a $\phi = 2.1$ flame. The data shown here have not been corrected for microphone response. When the frequency response of the microphone element is considered, it becomes clear that a significant proportion of the energy of the photoacoustic signal is present in the second harmonic, exceeding that of the first harmonic, highlighting the highly non-linear nature of the photoacoustic signal. It is likely that there is also a significant proportion of the energy in further harmonics; however, these could not be measured due to the low sensitivity of the microphone at frequencies above 20 kHz.

The frequency response has been characterised at a range of locations in the flame. Figure 5 shows both the first and second harmonic outputs from the lock-in amplifier for a range of heights above the burner in a $\phi = 2.48$ flame, corrected for microphone frequency response. It can be seen

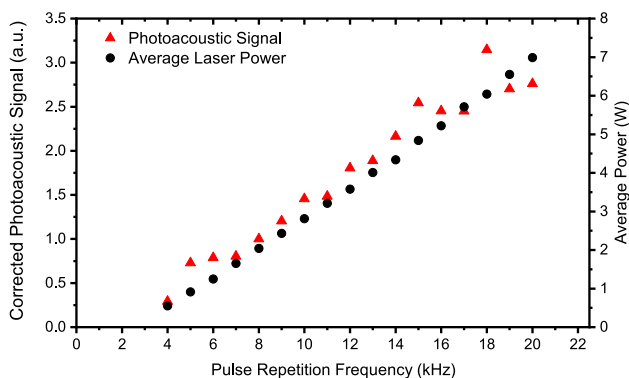


Fig. 3 Measured photoacoustic signal and average laser power as a function of pulse repetition frequency

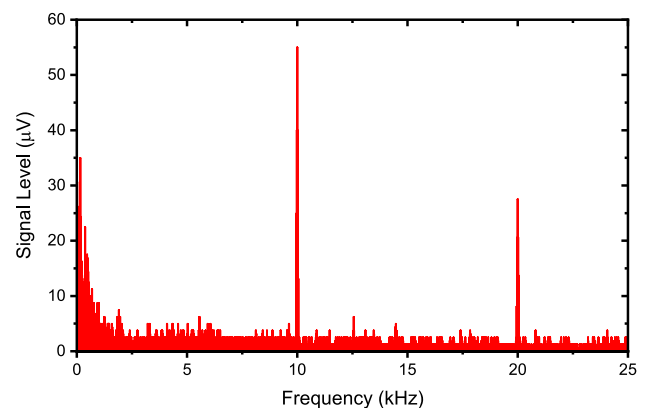


Fig. 4 FFT of raw (uncorrected) microphone output for a 10 kHz pulse repetition rate, using a fluence of 362 mJ cm^{-2}

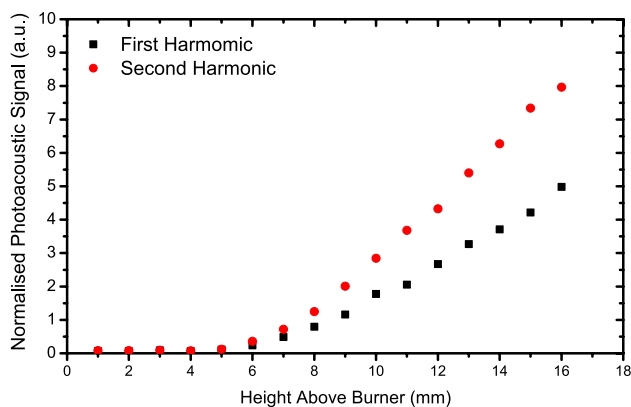


Fig. 5 First and second harmonic components of photoacoustic signal, recorded at various heights above the burner surface in a $\phi = 2.48$ flame

that the 1st/2nd harmonic ratio is roughly constant with height for positions greater than 7 mm above the burner, where soot is known to be present. This demonstrates that the second harmonic signal provides an equivalent measure of the photoacoustic signal. Nevertheless, the first harmonic signal (with 10 kHz rep-rate excitation) has been used for the evaluation of soot profiles due, in part, to the better sensitivity of the microphone at that frequency. Photoacoustic measurement of soot has previously been shown to agree well with LII in terms of relative signal levels [8].

Calibration of the photoacoustic signal to soot volume fraction was achieved by extinction measurements using a low-power (< 20 mW) 1064-nm diode laser. To improve the sensitivity of the extinction measurements, a 100 kHz sinusoidal modulation was applied to the laser drive current, thus producing a sinusoidal variation in the intensity of the laser output. The transmitted intensity was monitored using an InGaAs photodiode and de-modulated using the lock-in amplifier. Extinction measurements were performed at a range of positions above the burner surface in the $\phi = 2.48$ flame. The absorption path length for the extinction measurements was assumed to be the diameter of the porous plug. This will introduce a slight uncertainty but seems reasonable based on a radial LII profile recorded at 15 mm above the burner in similar flames presented in our previous work [8]. The measured extinction coefficient k_{ext} is related to the soot volume fraction f_V according to [12]:

$$k_{\text{ext}} \approx k_{\text{abs}} = f_V \frac{6\pi E(m)}{\lambda}, \quad (1)$$

where k_{abs} is the soot absorption coefficient, λ is the wavelength of the incident light, and $E(m)$ is the soot absorption function. The choice of the correct value for $E(m)$ is the dominant source of error for this calibration technique; it has been the subject of numerous recent publications, and has been shown to vary significantly with soot maturity [13].

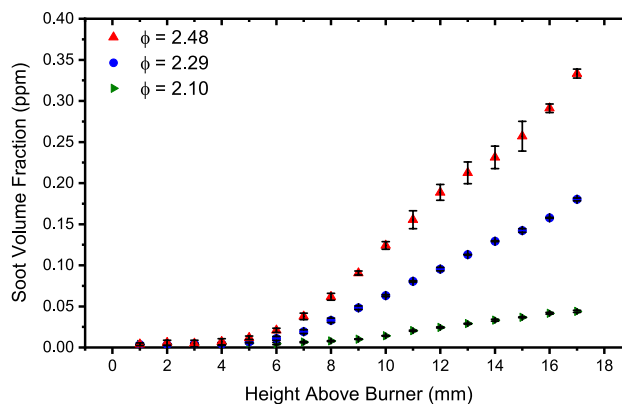


Fig. 6 Vertical profiles of soot distribution for a range of flames of different equivalence ratios ($\phi = 2.1$ to $\phi = 2.48$) (error bars represent the standard error in three measurements)

A value of $E(m) = 0.39$, as suggested by Desgroux et al. [14], has been used here. The photoacoustic profile for the same flame was scaled to the soot volume profile measured by extinction using a least squares fit algorithm in Matlab.

Figure 6 shows the measured photoacoustic signal as a function of height above burner for flames with a range of different equivalence ratios ($\phi = 2.1$ to $\phi = 2.48$). As expected, there is a clear trend of increasing photoacoustic signal as the equivalence ratio, and hence soot volume fraction, is increased. In all the flames there is negligible signal at positions below 6 mm above the burner. This is in agreement with LII measurements made in ethylene–air flat flames under the same conditions which indicate that solid soot particles begin to occur from 7 mm above the burner surface [15]. In general, the profiles of soot volume fraction with height above burner as well as with equivalence ratio tends to agree with these previous LII measurements [15], thus highlighting the applicability of photoacoustic soot measurement in radially uniform systems.

To obtain a measurement of the stability and sensitivity of the photoacoustic technique, the signal level was logged for 30 minutes, with a 0.5 Hz sample frequency (equivalent to the lock-in amplifier time constant). Some increasing linear drift as well as a number of short-term downward fluctuations were observed in the signal level. The short-term fluctuations likely correspond to perturbations to the flame caused by disturbances to the ambient air currents surrounding the burner. It is important to note that the effect of such fluctuations on the measured signal will have already been reduced by the comparatively long time constant used for the lock-in amplifier. Figure 7 shows the calculated Allan–Werle deviation for this data series. The effect of the aforementioned linear drift results in an optimum integration time of ≈ 100 s with a corresponding sensitivity (3σ) of 3 ppb. As the data are already integrated for a period of 2 s during the lock-in process there is not a substantial improvement in sensitivity from averaging

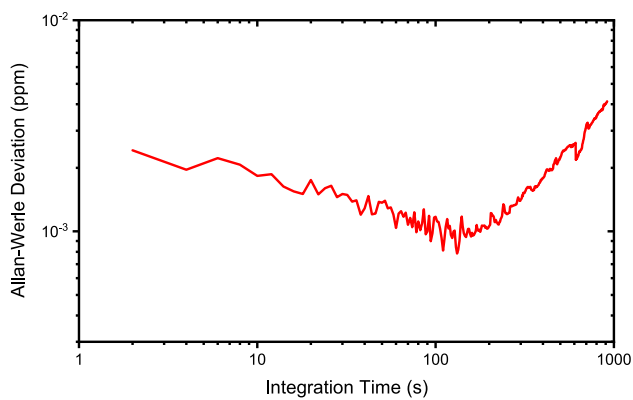


Fig. 7 Allen–Werle deviation of photoacoustic signal recorded at 2 s intervals for a measurement position 15 mm above the burner surface in a $\phi = 2.1$ flame

the signal ($\approx 70\%$ relative improvement). This is apparent from the relatively shallow gradient preceding the minimum on the Allan–Werle plot. We also note that slight flame instabilities, therefore, result in a less favourable sensitivity than the true capability of the technique.

A potential source of error in the photoacoustic measurements compared to LII is that any absorption of the laser energy, not only that due to the presence of soot (e.g. rovibrational absorption from gaseous species), will also produce a photoacoustic signal. There are a number of other factors which may have an effect on the photoacoustic signal which have not been considered here such as the temperature of the gas medium surrounding the soot particle which will effect the rate of heat transfer from the particle following heating by the laser. Other factors which may have an effect on the acoustic signal include the pressure and speed of sound in the surrounding gas medium. It should also be noted that variations in the composition of the bath gas (e.g. through the introduction of diluents, to the fuel–air mixture supplied to the burner) can alter the rate of heat transfer from the soot particle to the gas; although this may cause some variation in resulting photoacoustic signal, the cooling of the soot particles may well be so rapid that this effect is minor. Further work would be required to quantify any effect on the signal calibration. The standard error in the extinction measurements, which was approximately 30 ppb, combined with the uncertainty in choosing the correct value of $E(m)$ for calibration represents the main source of uncertainty with the current photoacoustic measurement technique.

4 Conclusion

To conclude, we have demonstrated a new photoacoustic technique for the measurement of soot distribution using a high-repetition-rate pulse fibre laser. The behaviour of the

acoustic signal with increasing laser fluence was shown to be very similar to that which is observed optically using LII, indicating that the particles have been heated to a sufficient temperature for sublimation to occur. The increasing level of this plateau with repetition rate is attributed to the transient nature of the pressure wave resulting from the pulsed laser excitation. The detection limit (3σ) of the technique was determined to be a soot volume fraction of 3 ppb following ≈ 100 s of integration.

Acknowledgements The authors gratefully acknowledge SPI Lasers for the loan of a redENERGY G4 laser.

Funding This work was supported by an EPSRC Platform Grant (number: EP/P001661/1). G. S. Humphries was supported by an EPSRC Doctoral Prize (University of Strathclyde, 2016).

Open Access This article is distributed under the terms of the Creative Commons Attribution 4.0 International License (<http://creativecommons.org/licenses/by/4.0/>), which permits unrestricted use, distribution, and reproduction in any medium, provided you give appropriate credit to the original author(s) and the source, provide a link to the Creative Commons license, and indicate if changes were made.

References

1. K. Gerdes, R. Stevens, T. Fout, J. Fisher, G. Hackett, W. Shelton, Current and Future power generation technologies: pathways to reducing the cost of carbon capture for coal-fueled power plants. *Energy Procedia* **63**, 7541 (2014). <https://doi.org/10.1016/J.EGYPRO.2014.11.790>
2. R. Niranjana, A.K. Thakur, The toxicological mechanisms of environmental soot (black carbon) and carbon black: focus on oxidative stress and inflammatory pathways. *Front. Immunol.* **8**, 763 (2017). <https://doi.org/10.3389/fimmu.2017.00763>
3. J. Hansen, L. Nazarenko, Soot climate forcing via snow and ice albedos. *Proc. Natl. Acad. Sci. USA* **101**(2), 423 (2004). <https://doi.org/10.1073/pnas.2237157100>
4. H. Michelsen, Probing soot formation, chemical and physical evolution, and oxidation: a review of in situ diagnostic techniques and needs. *Proc. Combust. Inst.* **36**(1), 717 (2017). <https://doi.org/10.1016/J.PROCI.2016.08.027>
5. L.A. Melton, Soot diagnostics based on laser heating. *Appl. Opt.* **23**(13), 2201 (1984). <https://doi.org/10.1364/AO.23.002201>
6. C. Schulz, B.F. Kock, M. Hofmann, H. Michelsen, S. Will, B. Bougie, R. Suntz, G. Smallwood, Laser-induced incandescence: recent trends and current questions. *Appl. Phys. B Lasers Opt.* **83**(3), 333 (2006). <https://doi.org/10.1007/s00340-006-2260-8>
7. S. Will, S. Schraml, K. Bader, A. Leipertz, Performance characteristics of soot primary particle size measurements by time-resolved laser-induced incandescence. *Appl. Opt.* **37**(24), 5647 (1998). <https://doi.org/10.1364/AO.37.005647>
8. G.S. Humphries, J. Dunn, M.M. Hossain, M. Lengden, I.S. Burns, J.D. Black, A simple photoacoustic method for the in situ study of soot distribution in flames. *Appl. Phys. B* **119**(4), 709 (2015). <https://doi.org/10.1007/s00340-015-6132-y>
9. D. McCormick, J.D. Black, Y. Feng, J. Nilsson, K.B. Ozanian, High-sensitivity in situ soot particle sensing in an aero-engine exhaust plume using long-pulsed fiber-laser-induced

- incandescence. *IEEE Sens. J.* **16**(8), 2674 (2016). <https://doi.org/10.1109/JSEN.2015.2507702>
10. G.S. Humphries, I.S. Burns, M. Lengden, Application of continuous-wave cavity ring-down spectroscopy to laminar flames. *IEEE Photon. J.* **8**(1), 1 (2016). <https://doi.org/10.1109/JPHOT.2016.2517575>
 11. E. Cenger, A. Bennett, W.L. Roberts, Investigations of the long-term effects of LII on soot and bath gas. *Aerosol Sci. Technol.* **51**(12), 1354 (2017). <https://doi.org/10.1080/02786826.2017.1368444>
 12. H. Michelsen, C. Schulz, G. Smallwood, S. Will, Laser-induced incandescence: particulate diagnostics for combustion, atmospheric, and industrial applications. *Prog. Energy Combust. Sci.* **51**, 2 (2015). <https://doi.org/10.1016/J.PECS.2015.07.001>
 13. N.E. Olofsson, J. Simonsson, S. Török, H. Bladh, P.E. Bengtsson, Evolution of properties for aging soot in premixed flat flames studied by laser-induced incandescence and elastic light scattering. *Appl. Phys. B* **119**(4), 669 (2015). <https://doi.org/10.1007/s00340-015-6067-3>
 14. P. Desgroux, X. Mercier, K.A. Thomson, Study of the formation of soot and its precursors in flames using optical diagnostics. *Proc. Combust. Inst.* **34**(1), 1713 (2013). <https://doi.org/10.1016/j.proci.2012.09.004>
 15. R. Hedef, K.P. Geigle, W. Meier, M. Aigner, Soot characterization with laser-induced incandescence applied to a laminar premixed ethylene-air flame. *Int. J. Therm. Sci.* **49**(8), 1457 (2010). <https://doi.org/10.1016/J.IJTHERMALSCI.2010.02.014>

Publisher's Note Springer Nature remains neutral with regard to jurisdictional claims in published maps and institutional affiliations.